CFD Simulation Of an Industrial Scale Catalyst Lift Pot In Persian Gulf Star Gas Condensate Refinery Company

Mehdi Hashemi Pour[1] *,Hamed Fathi[2], Mohsen Asadi[3], Hamed Doshmanfana[4]

1,2,3,4 Persian Gulf Star Gas Condensate Refinery Company, Bandar Abbas, Hormozgan, Islamic Republic Of Iran
MehdiHashemipour.che@gmail.com

Abstract

The aim of this study is to simulate a Catalyst Flow Pattern in lift pot of CCR (continues catalyst regeneration) unit of Persian Gulf Star Gas Condensate Refinery Company. The lift pot is simulated with computational fluid dynamic methods. After choosing a suitable mesh grid for lift pot and checking independency, the impact of the change in primary and secondary mass flow rate of hydrogen on catalyst lifting is investigated. In this case hydrogen gas used for lifting catalyst in lift pot. K-Epsilon model is used for turbulence simulation of flow and two phases flow is simulated using Granular Eulerian-Eulerian approach. Three cases were examined but in each three cases total mass flow rate was constant an then we investigate the flow field, catalyst particles velocity and catalyst concentration distribution. Results showed with rise of secondary mass flow rate the volume fraction of catalyst in lift line increase. If secondary gas velocity was not adequate to fully fluidize the catalyst, therefore, resulting in a very poor mixing.

Key words: CFD Simulation, Flow Pattern, Catalyst lifting, Lift Pot, CCR unit

1. Introduction

Bandar Abbas Gas Condensate Refinery includes of three Octanizer & CCR (Unit numbers 02, 52, and 72) which are totally similar in regard of main process scheme.
The capacity of the present Octanizer unit (OCT) is 45,000 Barrels per stream day (for one train – three trains in the whole). The Octanizer unit produces a reformate with research octane number of 100 and benzene content < 1.5 vol%.
The purpose of the Octanizer unit is to produce:

- A high octane reformate
- A hydrogen rich gas for use in Isomerization, Kerosene Hydrotreated, Gasoil Hydrotreated, Sulfur Recovery Unit, Naphta Hydrotreated, and regeneration units
- A LPG cut routed to the LPG recovery unit

1- Shift Supervisor of NHT, OCT and CCR units, Persian Gulf Star Gas Condensate

This process utilizes moving catalyst bed technology. The hydrotreated naphtha feed stream is reacted at very low pressure (4.4 , 3.9 , 3.5 barg) in three adiabatic reactors over a moving bimetallic catalyst bed in a hydrogen environment. Catalyst is withdrawn at a fixed rate from the

reaction section and is regenerated in a continuous catalyst regeneration unit (CCR) before returning to the reaction section. This continuous regeneration of the catalyst allows the catalyst beds to operate with a low coke deposit, thereby ensuring maximum catalyst performance at the process operating conditions.[1]

Catalyst flow in lifts

The catalyst flow is adjusted as follows : the total flowrate of the lift gas must remain as steady as possible since any change in this flow will affect the velocity of the catalyst in the lift line. This flowrate must be checked carefully because a too high velocity may lead to a high rate of catalyst attrition.

Hydrogen gas that used for catalyst lifting is divided into two streams :

- The primary gas, which initiates the lift operation.
- The secondary gas, which governs the catalyst flow.

Within the proper operating range, the rate of catalyst flow is proportional to the secondary flowrate of gas. When the secondary gas is stopped no catalyst can be lifted.

One of the key aspects of the CCR is the catalyst circulation between the reactor and regenerator. It is important to maintain a sufficient rate of circulations as inefficient catalyst circulations may lead to retardation of reforming reaction rate. Generally, to compensate for the reduced reaction rate, make up catalyst must be added which affects the economy of the whole plant. The catalyst circulation is controlled by the lift engagers situated at the bottom of the reactor and regenerator. The efficiency of the lift pot in terms of catalyst lift rate depends on various operating and design parameters such as the lift gas velocity, lift line gap and catalyst feed rate. The hydrodynamics of the gas solid flow plays an important role in governing the performance of the lift engager. Higher gas velocities in the lift line can result in excessive catalyst attrition, whereas low gas velocities can produce an unstable lifting.

In these CFD models have been discussed in detail by Van der Hoef et al. [2] and van Wachem et al. [3]. Based on the treatment of the solid phase, the CFD models can be primarily divided into two categories, namely, the Eulerian–Lagrangian and the Eulerian–Eulerian approaches. In the Eulerian–Lagrangian approach, the gas phase is continuous and the solid phase is represented as a collection of discrete particles that obey the second law of Newton. The accuracy of simulation in the Eulerian–Lagrangian model is dependent on the number of particles tracked, which in turn is dependent on the computational resources employed. Therefore, for realistic industrial scale simulations, this approach is computationally intensive. In the Eulerian–Eulerian model, both the solid and gas phases are represented as continuous and interpenetrating. This representation is computationally less intensive and is well suited for modelling of industrial scale flows [4].

In the Eulerian–Eulerian model, basic transport equations in terms of mass and momentum conservation are written for each phase using an averaging. Enwald et al. [5] have discussed various averaging techniques for the formulation of the two-fluid model equations. The ensemble averaging of local instantaneous balances for each phase is used in formulating the averaged governing equations that are used in the CFD code such as FLUENT. For each phase, the continuity and momentum balance equations are written.

2. Hydrodynamic modelling of gas–solid flows

The hydrodynamic study is simulated using Granular-Eulerian multiphase model. Each phase, in this model, is treated as an interpenetrating continuum represented by a volume fraction at each point of the system. The Reynolds averaged mass and momentum balance equations are solved for each of the phases. The governing equations are given below:

Continuity equation:

$$\frac{\partial}{\partial t}(\propto_q \ \rho_q)+\nabla.(\propto_q \ \rho_q \vec{u_q}) = 0 \qquad (1)$$

$$\frac{\partial}{\partial t}(\propto_q \ \rho_q \vec{u_q})+\nabla.(\propto_q \ \rho_q \vec{u_q} \vec{u_q}) = \propto_q \ \nabla P + \nabla.\overline{\overline{\tau_q}} + \propto_q \ \rho_q \vec{g}$$

$$+(\vec{F_{td}} + \vec{F_q} + \vec{F_{lift,q}} + \vec{F_{vm,q}})+C \qquad (2)$$

Where q is 1 or 2 for primary or secondary phase respectively, $\propto$ is volume fraction, ρ is density, $\vec{u}$ is velocity vector, P is pressure and is shared by both the phases, $\overline{\overline{\tau}}$ is the stress tensor because of viscosity and velocity fluctuation, g is gravity, $\vec{F_{td}}$ is force due to turbulent dissipation, $\vec{F_q}$ is external force, $\vec{F_{lift,}}$is lift force, $\vec{F_{vm}}$ is virtual mass force and F_{12} is interphase interaction force.

The stress-strain tensor is due to viscosity and Reynolds stresses that include the effect of turbulent fluctuation. Using the Boussinesq's eddy viscosity hypothesis the closure can be given to the above momentum transfer equation. The stress strain tensors for gas and solid phase are given by Eqs. (3) and (4) respectively:

$$\overline{\overline{\tau_g}} = \propto_g \ \mu_g(\nabla \vec{v_g} + \nabla \vec{v_g}^T) + \propto_g (\lambda_g - \frac{2}{3}\mu_g) \nabla.\vec{v_g} \overline{\overline{I}} \qquad (3)$$

$$\propto_s \overline{\overline{\tau_s}} = -P_s \overline{\overline{I}} + \propto_s \ \mu_s(\nabla \vec{v_s} + \nabla \vec{v_s}^T) + \propto_s (\lambda_s - \frac{2}{3}\mu_s) \nabla.\vec{v_{sq}} \overline{\overline{I}} \qquad (4)$$

Where μ is the shear viscosity, λ is bulk viscosity and $\overline{\overline{I}}$ in the unit stress tensor.

2.CFD Method

3D computational fluid dynamic (CFD) simulations was carried out in order to model the behavior of lift pot of catalyst in CCR unit. The mesh geometry of the lift pot which was created using

Gambit 2.3 as shown in fig.2a and Fluent version 6.3 was used for solving a set of nonlinear equations formed by discretization of the continuity, the particle mass balance and momentum equations. A computational grid consisting of four part: A Primary nozzle that work is lifting the catalyst particle with hydrogen mass flow rate, an inlet line of hydrogen that fluidize the catalyst particles in front of primary nozzle, a catalyst transfer line that is top of primary nozzle, a lift pot volume that catalyst particle free fall into there were used in the four parts that consisted of about 400000 tetrahidral nods. The dimensions of the lift pot geometry shown in Fig.1. In this work study 76% of the lift pot volume is filled with catalyst particles with diameter of 0.008 mm. The physical properties of solid and gas phase are presented in Table 1. An Granular-Eulerian Multi Fluid Model coupled and standard-k-ε model was selected for turbulency. Standard no-slip boundary condition was considered for all solid surfaces. In this word study we investigate mass flow rate of primary and secondary lifting gas, on hydrogen flow pattern, catalyst flow pattern and
catalyst velocity. To do this we considered three different case that the mass flow rate of primary and secondary lifting gas in each model shown in table2.

Table 1. The properties of solid and gas phases

Type / Shape	Density (kg/m3)	Average size (mm)	Solid loading (x_v)
Catalyst particles	650	0.008	67% vol
Hydrogen	Density (kg/m3)	Viscosity (pa.s)	
	0.08189	8.411×10^{-6}	

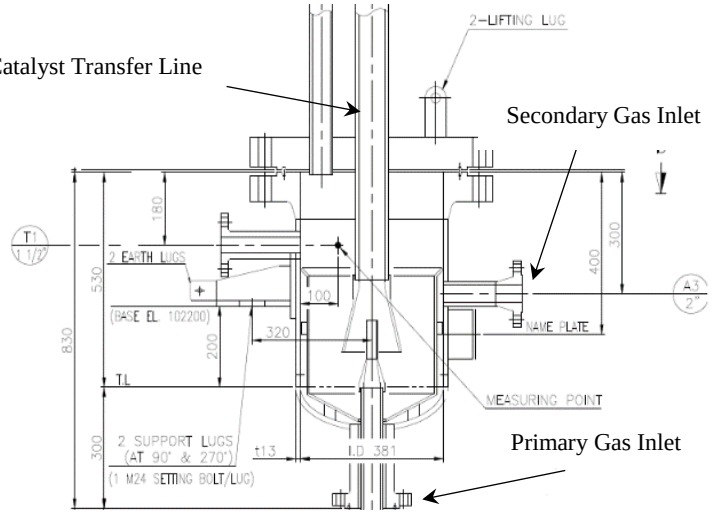

Figure 1. The dimensions of the lift pot geometry

Table 2. The mass flow rate of lifting gas in each model

Mass flow rate of lifting gas(Kg/hr)	Case. 1	Case. 2	Case. 3
Primary	73.3	36.7	20
Secondary	36.7	73.3	90

Sum of primary and secondary	110	110	110

1. Results and discussion

The initial catalyst bed was patched with packed solids (volume fraction 0.67) up to the entrance of the lift line as shown in Fig. 2b and simulations were commenced in an unsteady manner.

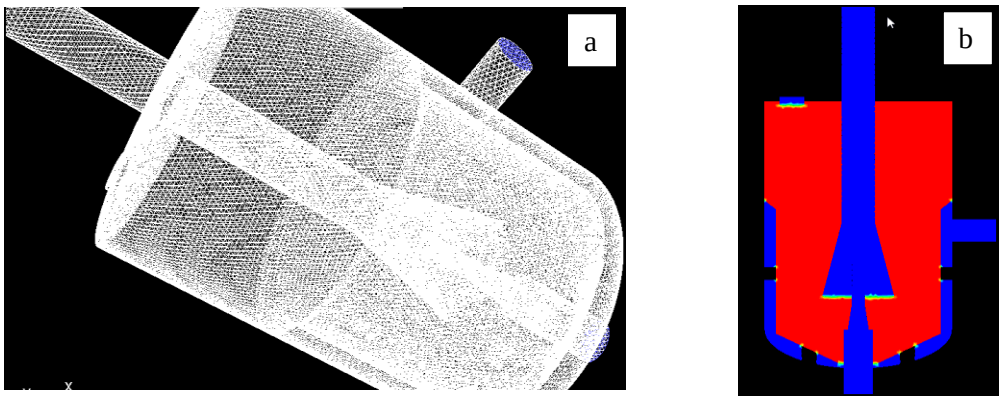

Figure 2. (a) The mesh geometry of the lift pot which was created using Gambit 2.3.(b) The initial catalyst bed was patched with packed solids

A. Flow Field

Fig. 3 shows the snapshots of catalyst volume fraction contour and catalyst velocity vectors on axis plane, for the case (2) simulation. It was observed that the catalyst falls though the inlet with an increasing velocity and decreasing volume fraction under the effect of gravity and the convective effect of the secondary gas (Fig. 3a and b). The secondary gas velocity reduces considerably after passing through the baffle region due to the sudden increase in the cross sectional area (Fig. 3b). It appeared that if secondary gas velocity was not adequate to fully fluidize the catalyst, therefore, resulting in a very poor mixing. Similarly, the primary gas immediately changed its direction upwards after entering the vessel and thus lifting the catalyst in the lift line although without any interaction with the bulk of solids in the equipment (Fig. 3b).

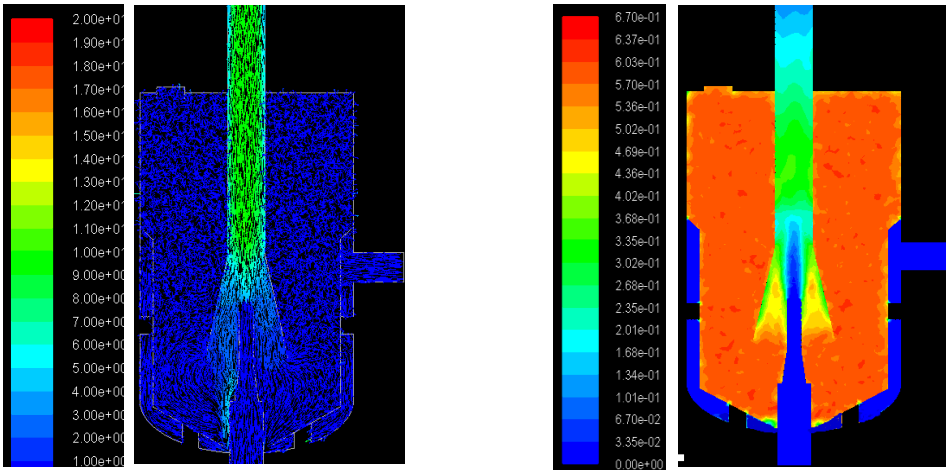

(a) (b)

Figure 3. Snap shots of (a) Catalyst velocity vectors and (b) Catalyst volume fraction contour For Case2 Which is the primary and secondary lift gas mass flow rate in equal order 73.3 and 36.7 Kg/hr

B. Effect of Primary and Secondary lift gas velocity

The primary and secondary lift gas velocities are very critical parameters which not only affect the catalyst lift rate but also associated disturbances therein. To study the effect of the lift gas flow rate on the catalyst transportation in the lift line, the simulations with various flow rates of primary and secondary gases were conducted. The simulated lift gas velocities, flow rate and the resulting gas velocity in the lift line are shown in Fig. 4. Depending on the lift gas velocities, the catalyst velocity increased sharply to rate of the 25–50% of the primary lift gas velocity.

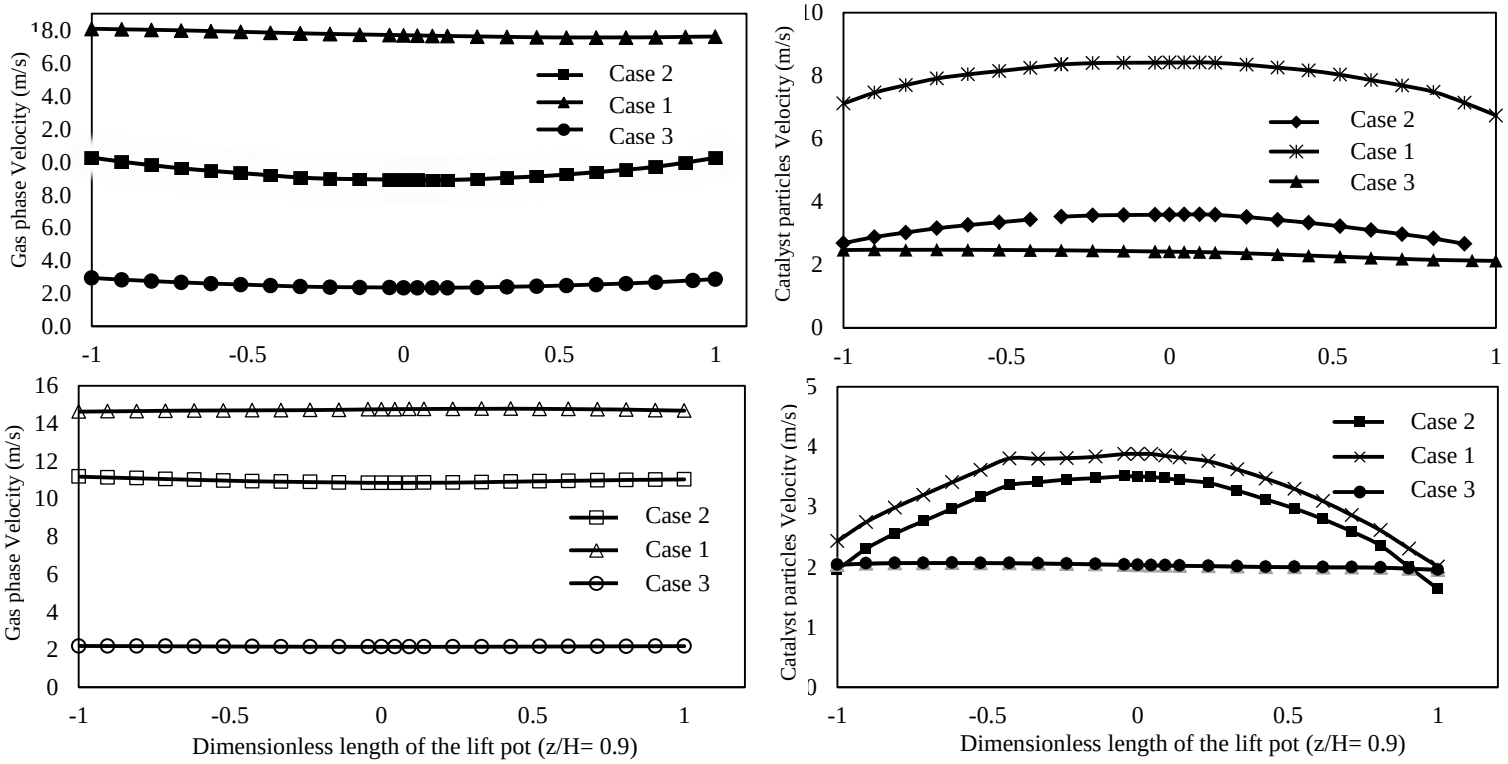

Figure 4. Velocity distribution of Gas and Catalyst phases in normalized length of lift line

As expected, an increase in the primary gas velocity increased the catalyst velocity in the lift line. A similar trend was observed for the increase in the secondary gas velocity. As shown in Fig. 4, the slip velocity profiles were found to be constant for the most part of the lift line except near the entrance. For all simulated cases, the predicted slip velocities were greater than the

terminal velocity of the catalyst particle. Fig.5 shown volume fraction distribution of catalyst particles in different length of lift line for each three cases. As shown fig.4a with rise of secondary mass flow rate the volume fraction of catalyst in lift line increase.

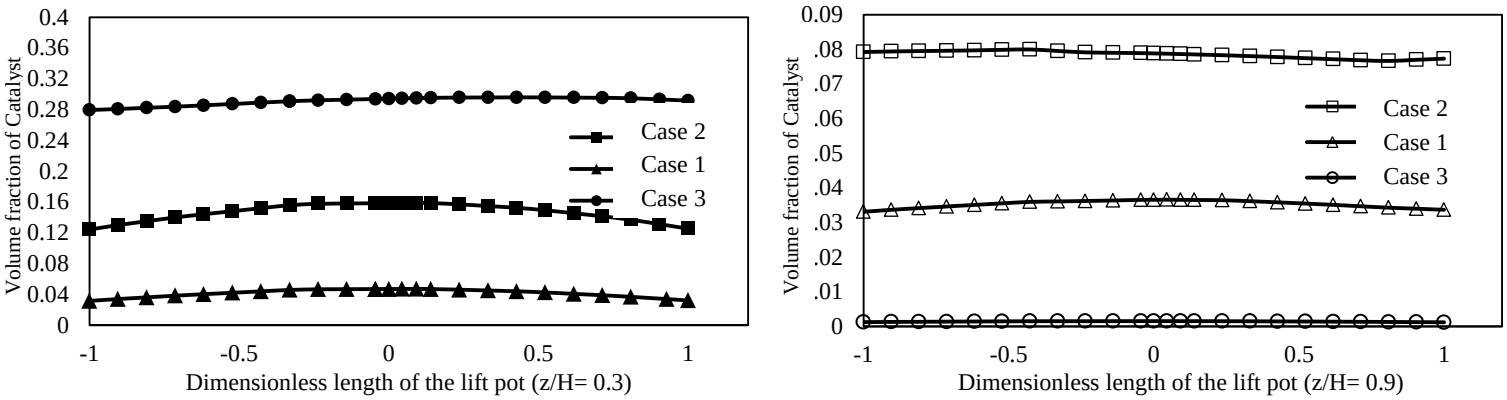

Figure 5. Volume fraction of catalyst particle in normalized length of lift line

2. Conclusions

The hydrodynamics of a lift pot, which is used in catalytic reformers, was investigated using a granular Eulerian–Eulerian model. A parametric study was also conducted by simulating three different cases having different combinations of the primary and secondary gas velocities. Flow field, solid particle velocity and solid concentration distribution are simulated. Results show that flow field is almost same for each three cases but amount of velocity is different. According to fig.5b by increasing the mass flow rate of secondary gas we have high density of catalyst particle near the top of primary nozzle and this cause is reason of not lifting of catalyst particles in high mass flow rate of secondary lift gas. As the best velocity of catalyst in lift line is nearly 2.5 – 3 m/s, combination of primary and secondary mass flow rate of case.2 is appropriate for lifting catalyst particle in CCR unit.

References

[1] M.A. Van der Hoef, M. van Sint Annaland, N.G. Deen, J.A.M. Kuipers, Numerical simulation of dense gas–solid fluidized beds: a multiscale modeling strategy Annual Review of Fluid Mechanics 70 (2008) 40–70.

[2] M.A. Van der Hoef, M. van Sint Annaland, N.G. Deen, J.A.M. Kuipers, Numerical simulation of dense gas–solid fluidized beds: a multiscale modeling strategy Annual Review of Fluid Mechanics 70 (2008) 40–70.

[3] B.G.M. van Wachem, A.E. Almstedt, Methods for multiphase computational fluid dynamics, Chemical Engineering Journal 96 (2003) 81–98.
[4] V.V. Ranade, Computational Flow Modeling for Chemical Reactor Engineering, Academic Press, 2001.
[5] H. Enwald, E. Peirano, A.E. Almstedt, Eulerian two-phase flow theory applied to fluidization, International Journal of Multiphase Flow 22 (1996) 21–66.

[6] B.G.M. van Wachem, A.E. Almstedt, Methods for multiphase computational fluid dynamics, Chemical Engineering Journal 96 (2003) 81–98.

[7] V.V. Ranade, Computational Flow Modeling for Chemical Reactor Engineering, Academic Press, 2001.
[8] H. Enwald, E. Peirano, A.E. Almstedt, Eulerian two-phase flow theory applied to fluidization, International Journal of Multiphase Flow 22 (1996) 21–66.